Submitted to the
International Europhysics Conference on High Energy Physics
Aachen, Germany, July 17–23, 2003

Abstract: 504 **HQCD, HP**

Multijet Production in DIS at ZEUS

Abstract

Multijet production rates in neutral current deep inelastic positron-proton scattering have been measured in a range of boson virtualities $10 < Q^2 < 5000\,\text{GeV}^2$. The data were taken at the ep collider HERA with center-of-mass-energy $\sqrt{s} = 318\,\text{GeV}$ using the ZEUS detector and correspond to an integrated luminosity of $82.2\,\text{pb}^{-1}$. Jets were identified using the longitudinally invariant k_T cluster algorithm. Measurements of differential multijet cross sections are presented as functions of jet transverse energy (E_T^{jet}), pseudorapidity (η^{jet}) and Q^2 with $E_T^{jet} > 5\,\text{GeV}$ and $-1 < \eta^{jet} < 2.5$. The data are compared to LO/NLO QCD calculations.

1 Introduction

In the quark-parton model (QPM), one-jet events consist of the struck quark and the proton remnant ($V^*q \longrightarrow q$, $V = \gamma$, Z^0). Events with 2 jets can be described at leading order (LO) by the $\mathcal{O}(\alpha_s)$ processes: boson-gluon fusion (BGF, $V^*g \longrightarrow q\bar{q}$) and QCD-Compton Scattering (QCDC, $V^*g \longrightarrow pq$), which give rise to two hard jets with opposite transverse momenta. Events with trijets can be seen as dijet processes with an additional gluon radiation or splitting of a gluon in a quark-antiquark pair, which are directly sensitive to $\mathcal{O}(\alpha_s^2)$ QCD effects.

A jet algorithm should distinguish as clearly as possible between the beam jet and the hard jets. Working in the Breit frame [1] is preferred, since it provides a maximal separation between the products of the beam fragmentation and the hard jets.

Recently the ZEUS collaboration has determined the strong coupling constant α_s and the gluon density in the proton from the inclusive jet and the dijet cross sections [2, 3] in the Breit frame. While these cross sections are directly sensitive to QCD effects in the order of $\mathcal{O}(\alpha_s)$, the trijet cross section is already of order $\mathcal{O}(\alpha_s^2)$ in leading order QCD. The measurement of trijet production is a direct test of higher order QCD calculations. In this analysis, the differential cross section for trijet events has been measured with the longitudinally invariant inclusive k_T algorithm [4] using a much larger event sample than the one previously available [5]. Another observable of interest is $R_{3/2}$, defined as the ratio of inclusive trijet cross section and the inclusive dijet cross section, since both experimental and some theoretical uncertainties in the ratio mostly cancel. The results of measurements are compared to predictions of MC models and perturbative QCD calculations in next-to-leading order in α_s.

2 Event Selection

The data used in this analysis were collected with the ZEUS detector in 1998-2000 when HERA operated with 920 GeV protons and 27.5 GeV positrons or electrons. An integrated luminosity of $65.5 \pm 1.5\,\mathrm{pb}^{-1}$ was taken with positrons and $16.7 \pm 0.3\,\mathrm{pb}^{-1}$ with electrons. A detailed description of the ZEUS detector can be found elsewhere [6]. In the present analysis the main components used were the central tracking detector (CTD) [7] and the ZEUS high-precision uranium-scintillator calorimeter (CAL) [8]. The ZEUS detector uses a three-level trigger system to select events online. For this analysis a DIS TLT trigger is used which is based on identifying the scattered electron. Electron and positron data were combined into one data sample which was then corrected for detector effects using a positron only MC.

The offline selection of DIS events is similar to the one used in a previous measurement of the inclusive jet and the dijet cross section [2, 3]. The characteristic signature of a DIS event is the scattered positron detected in the uranium-scintillator calorimeter. The kinematics of inclusive DIS are determined by the Q^2, x_{Bj}, and $y = Q^2/(sx_{Bj})$, where $\sqrt{s}$ is the positron-proton center-of-mass energy. The kinematic variables were calculated by a combination of methods: the electron method (e) [9], the double angle (DA) method [10] and the Jacquet-Blondel(JB) method [11].

The DIS event selection is based on the following requirements:

- $E_{e'} > 10\,\mathrm{GeV}$, $E_{e'}$ is the corrected energy of the scattered positron;
- $10\,\mathrm{GeV}^2 < Q^2 < 5000\,\mathrm{GeV}^2$;
- $y_e < 0.6$ and $y_{JB} > 0.04$, where y_e is reconstructed with the electron method and y_{JB} with the JB method;
- $\cos\gamma_{had} < 0.7$;
- $40 < \sum_i (E_i - P_{Zi}) < 60\,\mathrm{GeV}$, where the sum runs over all calorimeter energy deposits;
- a primary vertex position, determined from the tracks fitted to the vertex, in the range $\mid Z_{vertex} \mid < 50$ cm;
- the impact position of the scattered positron on the CAL satisfies $\mid X \mid > 13$ or $\mid Y \mid > 7$ cm

The kinematic range of the analysis is specified by:

$$0.04 < y < 0.6 \text{ and } \cos\gamma_{had} < 0.7 \text{ and } 10 < Q^2 < 5000\,\mathrm{GeV}^2$$

After these cuts, jets were reconstructed using the longitudinally invariant k_T algorithm [4] in the inclusive mode. The jet algorithm uses quantities defined in the Breit frame and with respect to the direction of the incoming proton: the transverse energy, E_T^i, the pseudorapidity, η^i, and the azimuthal angle, ϕ^i, of the object i. For each event the jet search was performed over all the CAL energy deposits using a combination of track and calorimeter information excluding the cells(tracks) associated with the scattered lepton. The tracks and calorimeter clusters are treated as massless energy-flow objects. The clustering of objects is done in the E_T recombination scheme. A detailed description of this procedure is given in [12]. The jet transverse energies were corrected for energy loss in the inactive material in front of the CAL using samples of MC generated events [13].

The jet phase space is defined by cuts on the jet pseudorapidity η_L in the laboratory frame and on the transverse jet energy $E_{T,B}$ in the Breit frame:

$$-1 < \eta_L < 2.5 \text{ and } E_{T,B} > 5\,\mathrm{GeV}$$

Events with two or more jets found in the Breit frame were selected by requiring the invariant mass cuts (jets ordered in E_T), for inclusive the trijet(dijet) sample:

$$M_{3jet}(M_{2jet}) > 25\,\mathrm{GeV}$$

After all cuts, there remained 38812 events with two or more jets and 14012 events with three or more jets.

3 Monte Carlo Simulation

Monte Carlo (MC) simulations were used to correct the data for detector acceptance and resolution. Two MC models were used to generate DIS events: ARIADNE 4.08 [14] and LEPTO 6.5 [15]. In ARIADNE, the QCD cascade is simulated using the colour-dipole model including the LO QCD diagrams. LEPTO, which uses the exact matrix elements to generate the hard process and the parton-shower model to simulate higher-order processes (MEPS model), was used as a systematic check of the final results. Both models use the Lund string model [16] of JETSET 7.4 [17, 18] for the hadronisation. To take into account first-order electroweak corrections, LEPTO and ARIADNE were interfaced with HERACLES 4.52 [19] using the DJANGO6 2.4 [20] program. The ZEUS detector response was simulated with a program based on GEANT 3.13 [21]. The generated events were passed through the simulated detector, subjected to the same trigger requirements as the data, and processed by the same reconstruction and offline programs.

Although the global event variables are well described by both ARIADNE and LEPTO. LEPTO gives the better overall description of the E_T and invariant mass distributions. Therefore, LEPTO was used as the default MC simulation to determine the corrections from the detector to producer hadron.

In addition, samples of events were generated without either Z^0 exchange or electroweak radiative events. These were used to correct the measured cross sections for these effects (QED Correction).

4 NLO QCD Calculations

The LO and NLO calculations are carried out in the $\overline{\mathrm{MS}}$ scheme for five massless quark flavors with the recent program NLOJET [22] using CTEQ6 [23] for the PDF. The calculations were corrected from original parton to produced hadron using LEPTO.

The renormalisation and factorization scale were both chosen to be $\bar{E}_T$. For dijets (trijets) $\bar{E}_T$ is the average E_T of the two (three) highest E_T jets in the acceptance region. The uncertainty on the NLO QCD predictions was estimated by varying the renormalisation and factorization scales from $\bar{E}_T/2$ to $2\bar{E}_T$.

5 Experimental and theoretical uncertainties

Experimental uncertainties originate from the jet-energy scale uncertainties and residual uncertainties in the event simulation. These uncertainties were estimated by correcting the data using the ARIADNE model and by varying the cuts in both data and MC simulation by an amount equal to the resolution on the relevant quantity. The biggest uncertainties come from using ARIADNE instead of LEPTO and varying the E_T cut on the jets. Not included in the plots is the uncertainty of 2.3% coming from the luminosity measurement.

6 Results

Figure 1 shows the cross section for inclusive dijet events as a function of the highest and second highest E_T jet. Figure 2 shows the cross section for the inclusive dijet events as a function of the highest and second highest η jet. For both measurements the data is well described by the NLO prediction. The different slopes of the calculations using different renormalisation scales cause them to cross for η of the most forward jet ≈ 0.25 which minimises the renormalisation scale uncertainty at this point.

A preliminary estimate of the PDF uncertainty made by substituting MRST2001 in place of CTEQ6 is generally smaller or equal in size to the renormalisation scale uncertainty.

Figures 3 and 4 show the measured cross section in E_T and η for inclusive trijet events. Again the data is well described by the NLO prediction.

Figure 5 shows the measured cross section as a function of Q^2 for both inclusive dijet and trijet events. For both the measurement is well described by the predictions. The small uncertainty in the dijet NLO prediction around $Q^2 = 400\,\mathrm{GeV}^2$ is again due to the NLO calculations crossing over at this point. Some systematic and the renormalisation scale uncertainties cancel when the ratio of trijet to dijet cross sections is calculated (figure 6). Even though the uncertainties are substantially reduced the measurement is still well described.

7 Summary

Differential dijet and trijet cross sections have been measured in neutral current deep inelastic scattering for $10 < Q^2 < 5000\,\mathrm{GeV}^2$ with high precision. These measurements were performed in a kinematic region where both theoretical and experimental uncertainties are small. The inclusive trijet cross section has been measured as a function of E_T, η and Q^2. The ratio $R_{3/2}$ of the inclusive trijet and inclusive dijet cross section has been measured as function of Q^2. The predictions of perturbative QCD in next-to-leading order give a good description of the trijet cross section and the ratio $R_{3/2}$ over the whole range of Q^2.

References

[1] R.P. Feynman, *Photon-Hadron Interactions*. Benjamin, New York, 1972;
K.H. Streng, T.F. Walsh, P.M. Zerwas, Z. Phys. **C**, 237 (1979).

[2] ZEUS Coll., J. Breitweg et al., Phys. Lett. **B 507**, 70 (2001).

[3] ZEUS Coll., S. Chekanov et al., Eur. Phys. J. **C 23**, 13 (2002).

[4] S.Catani et al., Nucl. Phys. **B406**, 187 (1993).

[5] H1 Coll., C. Adloff et al., Phys. Lett. **B 515**, 17 (2001).

[6] ZEUS Coll., U. Holm (ed.), *The ZEUS Detector*. Status Report (unpublished), DESY (1993), available on `http://www-zeus.desy.de/bluebook/bluebook.html`.

[7] N. Harnew et al., Nucl. Inst. Meth. **A 279**, 290 (1989);
B. Foster et al., Nucl. Phys. Proc. Suppl. **B 32**, 181 (1993);
B. Foster et al., Nucl. Inst. Meth. **A 338**, 254 (1994).

[8] M. Derrick et al., Nucl. Inst. Meth. **A 309**, 77 (1991);
A. Andresen et al., Nucl. Inst. Meth. **A 309**, 101 (1991);
A. Caldwell et al., Nucl. Inst. Meth. **A 321**, 356 (1992);
A. Bernstein et al., Nucl. Inst. Meth. **A 336**, 23 (1993).

[9] K.C. Höger, *Proc. Workshop on Physics at HERA*, W. Buchmüller and G. Ingelman (eds.), Vol. 1, p. 43. Hamburg, Germany, DESY (1992).

[10] S. Bentvelsen, J. Engelen and P. Kooijman, *Proc. Workshop on Physics at HERA*, W. Buchmüller and G. Ingelman (eds.), Vol. 1, p. 23. Hamburg, Germany, DESY (1992).

[11] F. Jacquet and A. Blondel, *Proceedings of the Study for an ep Facility for Europe*, U. Amaldi (ed.), p. 391. Hamburg, Germany (1979). Also in preprint DESY 79/48.

[12] D. Chapin, *A Measurement of Dijet Production in Neutral Current Deep Inelastic Scattering with ZEUS at HERA*. Ph.D. Thesis, Univeristy of Wisconsin, Madison, 2001. Unpublished.

[13] ZEUS Coll., J. Breitweg et al., Eur. Phys. J. **C 8**, 367 (1999).

[14] L. Lönnblad, Comp. Phys. Comm. **71**, 15 (1992).

[15] G. Ingelman, A. Edin and J. Rathsman, Comp. Phys. Comm. **101**, 108 (1997).

[16] B. Andersson et al., Phys. Rep. **97**, 31 (1983).

[17] M. Bengtsson and T. Sjöstrand, Comp. Phys. Comm. **46**, 43 (1987).

[18] T. Sjöstrand, Comp. Phys. Comm. **82**, 74 (1994).

[19] A. Kwiatkowski, H. Spiesberger and H.-J. Möhring, Comp. Phys. Comm. **69**, 155 (1992). Also in *Proc. Workshop Physics at HERA*, 1991, DESY, Hamburg.

[20] K. Charchula, G.A. Schuler and H. Spiesberger, Comp. Phys. Comm. **81**, 381 (1994).

[21] R. Brun et al., GEANT3, Technical Report CERN-DD/EE/84-1, CERN, 1987.

[22] Z. Nagy and Z Trocsanyi, Phys. Rev. Lett. **87**, 082001 (2001).

[23] J. Pumplin et al., Preprint hep-ph/0201195, 2002.

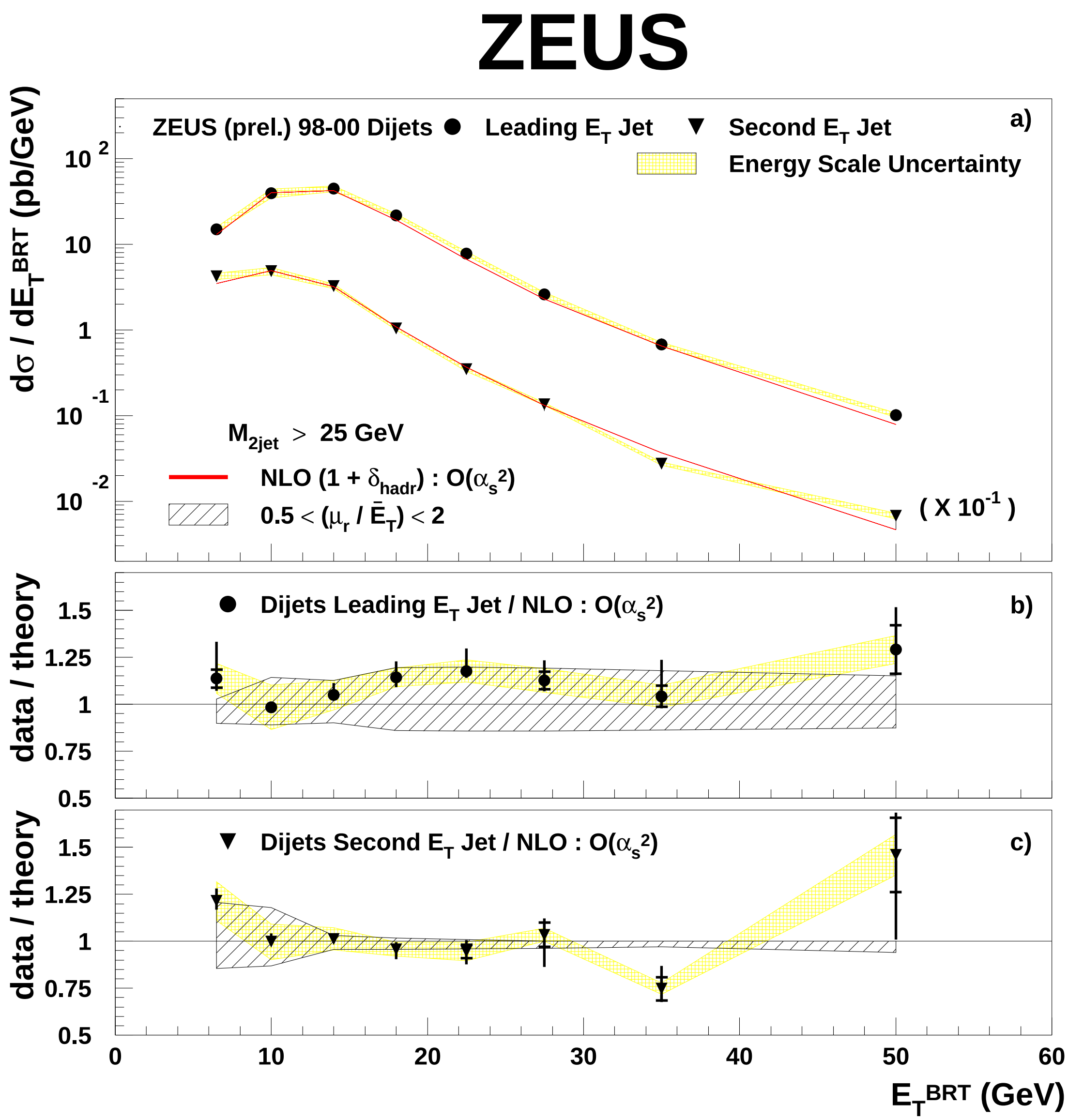

Figure 1: *The inclusive dijet cross sections as a function of E_T^{jet} with the jets ordered in E_T. The cross section of the second jet is scaled down for readability. The inner error bars represent the statistical uncertainties and the outer error bars represent the quadratic sum of all uncertainties. The yellow band indicates the calorimeter energy scale uncertainty. The predictions of perturbative QCD in next-to-leading order is compared to the data. b) and c) show the ratio of data over predictions. The shaded band represents the renormalisation scale uncertainty of the QCD calculation. The NLO is corrected from the parton to hadron level using correction factors obtained from parton and hadron level LEPTO. The correction are in general at the order of 8% except for the lowest E_T bins where they reach 20–30% and at the high E_T bins for the second jet where they go down to 2%.*

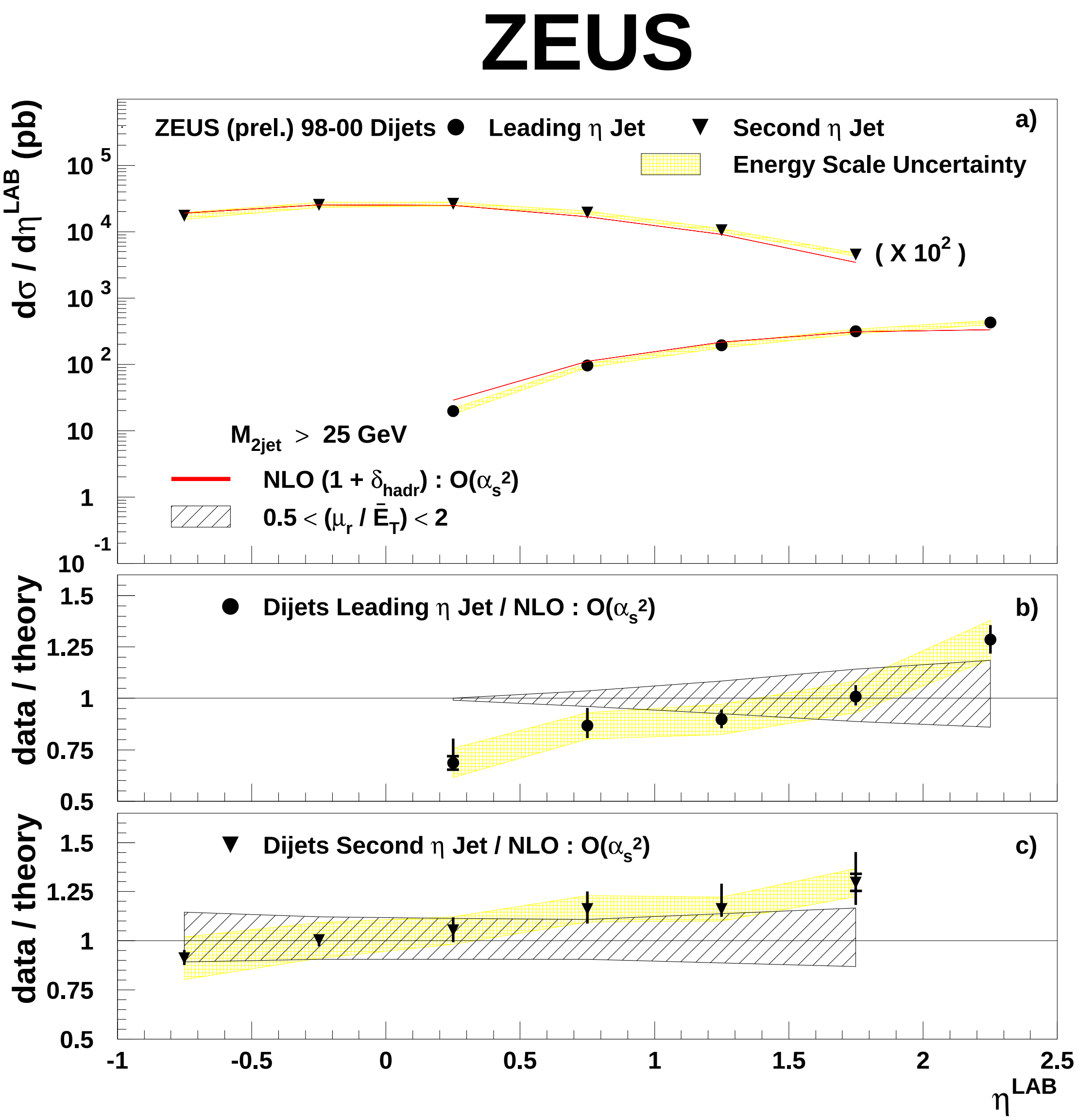

Figure 2: *The inclusive dijet cross sections as a function of η^{jet} with the jets ordered in η. The cross section of the second jet is scaled up for readability. The inner error bars represent the statistical uncertainties and the outer error bars represent the quadratic sum of all uncertainties. The yellow band indicates the calorimeter energy scale uncertainty. The predictions of perturbative QCD in next-to-leading order is compared to the data. b) and c) show the ratio of data over predictions. The shaded band represents the renormalisation scale uncertainty of the QCD calculation. The renormalisation scale uncertainty for the first jet goes to 0 because the NLO has different shapes for different scales. (cmp. figure 5) The hadronisation corrections are on the order of 10–20% except for the first jet in the forward bins where they go down to 5%.*

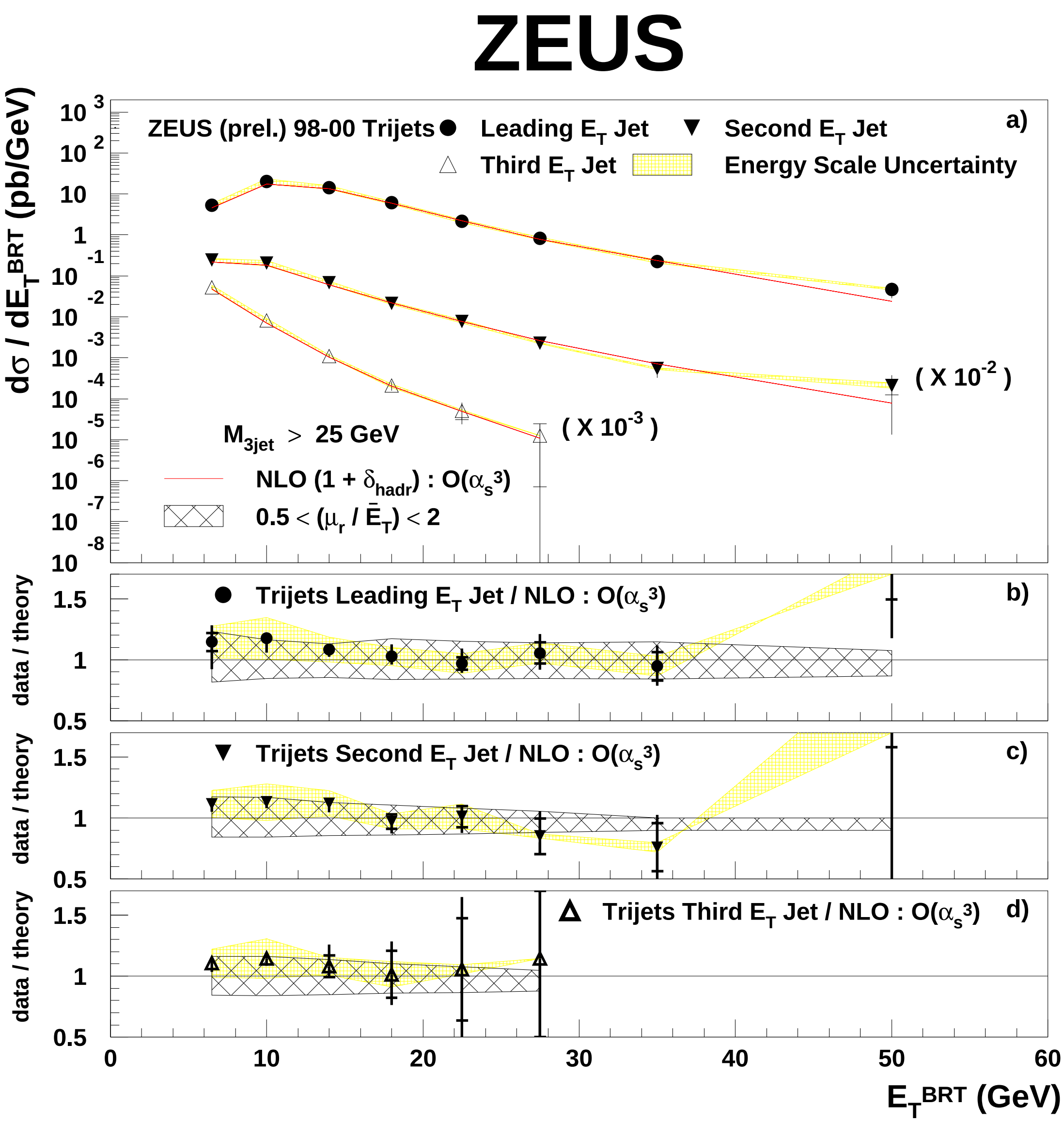

Figure 3: *The inclusive trijet cross section under the same conditions as figure 1. The hadronisation corrections are in the order of 20–30% except at high E_T bins for the third jet where they go down to 1%.*

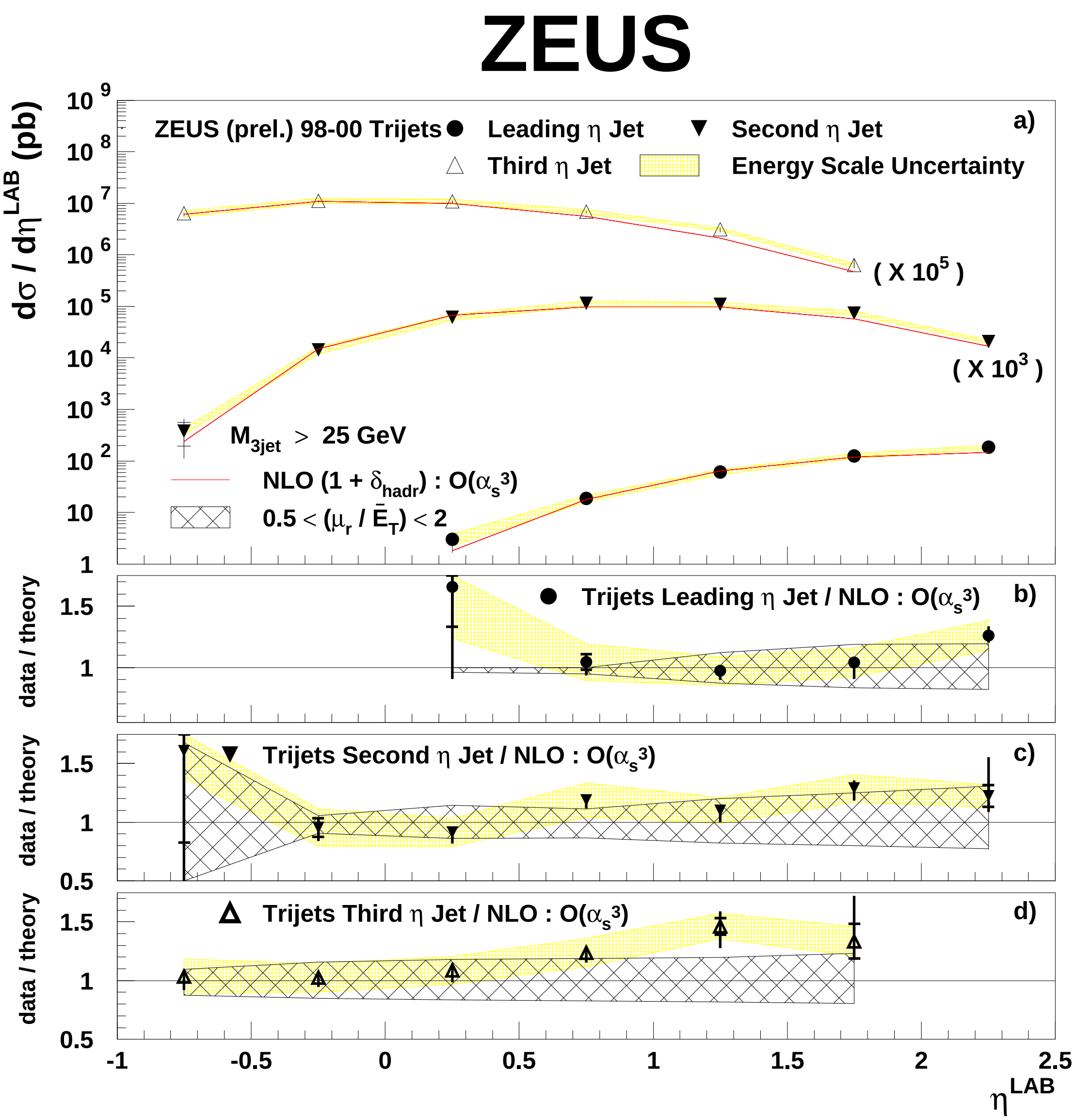

Figure 4: *The inclusive trijet cross section under the same conditions as figure 2. The renormalisation scale uncertainty for the first jet goes to 0 because the NLO has different shapes for different scales. (cmp. figure 5) The hadronisation corrections are in the order of 20–25% except in the backward bins where they go up to 40%.*

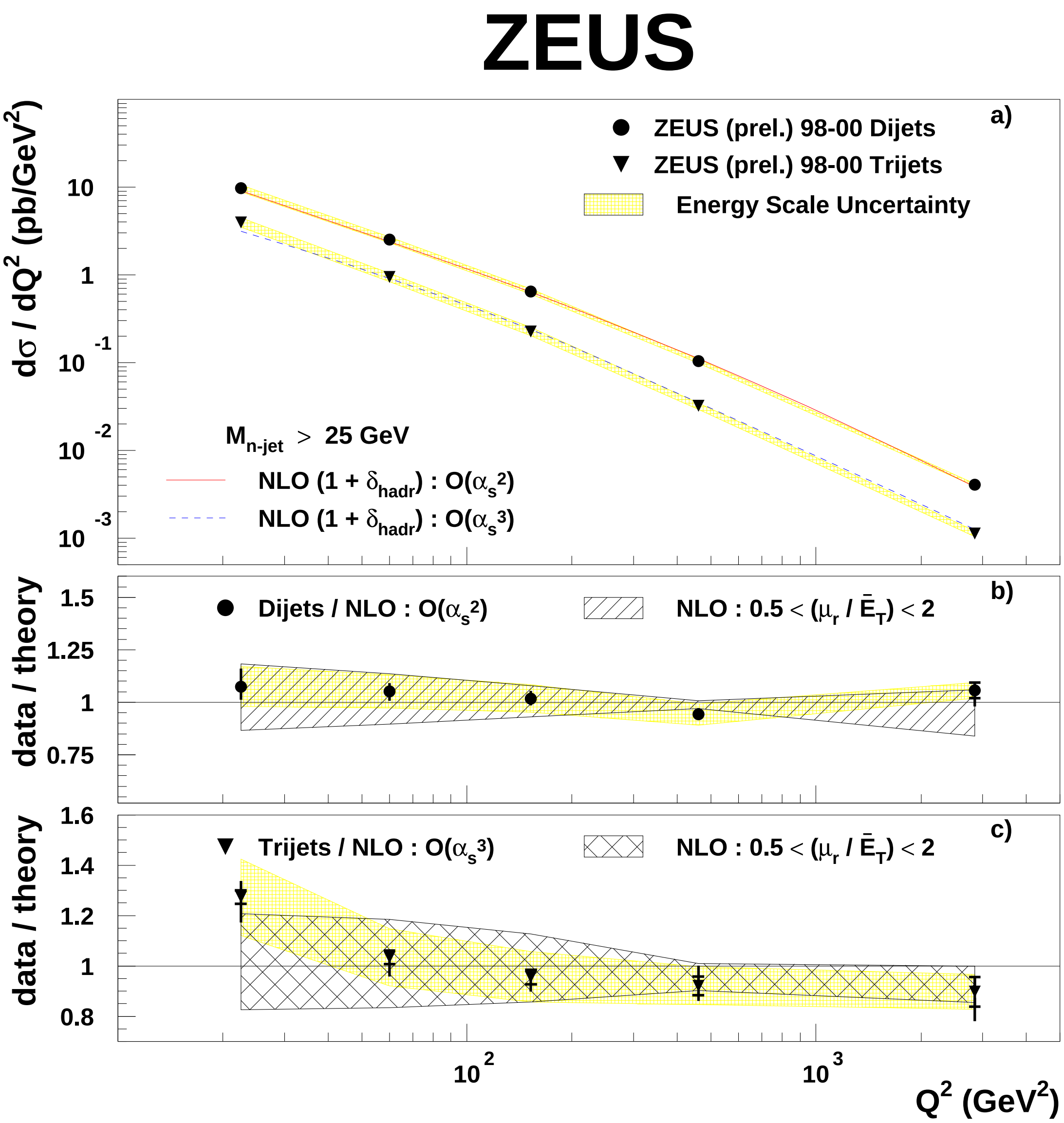

Figure 5: *The inclusive dijet and trijet cross sections as a function of Q^2. The inner error bars represent the statistical uncertainties and the outer error bars represent the quadratic sum of all uncertainties. The yellow band indicates the calorimeter energy scale uncertainty. The predictions of perturbative QCD in next-to-leading order is compared to the data. b) and c) show the ratio of data over predictions. The shaded band represents the renormalisation scale uncertainty of the QCD calculation. For the dijet cross section the renormalisation scale uncertainty gets smaller in the middle because changing the renormalisation scale changes the shape of the cross section and that's the point where they cross over. The hadronisation corrections for dijets are 10–15% and for trijets at the order of 25%.*

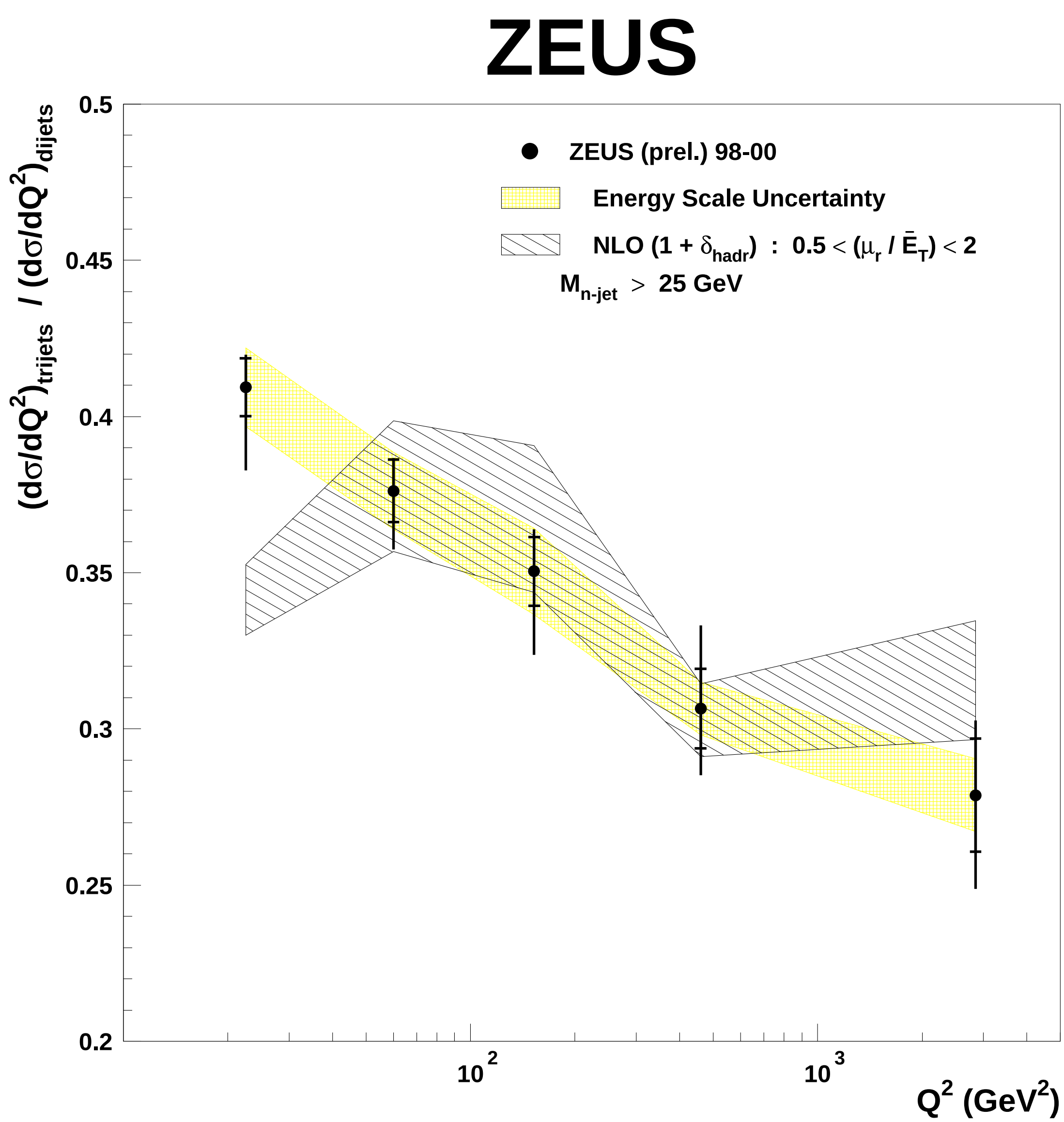

Figure 6: *The ratio of inclusive trijet over dijet cross sections as a function of Q^2. The predictions of perturbative QCD in next-to-leading order is compared to the data. The yellow band indicates the calorimeter energy scale uncertainty. The shaded band represents the renormalisation scale uncertainty of the QCD calculation.*